

# Simulation of the unsteady turbulent Ekman layer

B.C. BARR,<sup>a</sup> D.N. SLINN,<sup>a</sup> AND M.R. DHANAK<sup>b</sup>

<sup>a</sup>Department of Civil and Coastal, University of Florida, Gainesville, FL 32611

<sup>b</sup>Department of Ocean Engineering, Florida Atlantic University, Boca Raton, FL 33431

AGU Fall Meeting 2002

Poster OS52D-0258

Sponsored by the Office of Naval Research

## ABSTRACT

We investigate the role of an unsteady wind stress on a turbulent Ekman layer, using Large Eddy Simulations (LES). Analysis of the flow structure as well as the temporal and spatial dependence of the eddy viscosity is presented, highlighting the effect of the unsteadiness on modifying the depth of the Ekman layer.

It has previously been found that the tangential component of the Coriolis force, often neglected in geophysical applications, is significant at influencing the net properties of the Ekman layer, and can either increase or decrease the mixed layer depth depending on the wind direction and latitude. The current work suggests that the unsteady nature of wind on the ocean surface will complicate separating the Ekman component of circulation from observations.

The numerical method uses a pseudo-spectral Fourier technique for the horizontal plane, and a finite difference discretization in the vertical direction. The dynamic LES model is used for the subgrid closure. The domain is periodic horizontally with an aspect ratio of  $1 \times 1 \times 1.5$ .

## 1 Introduction

A turbulent Ekman layer created by an unsteady wind near the water surface is investigated using the method of numerical large-eddy simulations. This is a variation on the classic case of steady wind forcing.

### 1.1 Classic Ekman solution

The flow induced by a steady wind over the ocean surface was first investigated by Ekman in 1905. Assuming a balance between the pressure gradient, Coriolis force and viscous friction, with a constant vertical eddy viscosity, the steady-state solution for the velocity profile in the open ocean (northern hemisphere) can be written:

$$u = V_0 \cos\left(\frac{\pi}{4} + \frac{\pi}{D} z^*\right) \exp\left(-\frac{\pi}{D} z^*\right), \quad (1)$$

$$v = -V_0 \sin\left(\frac{\pi}{4} + \frac{\pi}{D} z^*\right) \exp\left(-\frac{\pi}{D} z^*\right). \quad (2)$$

Here  $u$  and  $v$  are the components of the mean horizontal velocity,  $z^*$  is the vertical coordinate directed downward,  $V_0 = \sqrt{2\pi\tau_0/Df\rho}$  is the amplitude of the surface velocity,  $D = \pi(2A_z/f)^{1/2}$  is the Ekman depth of exponential decay,  $\tau_0$  is the surface shear stress, and  $f = (1/2)\Omega \sin \lambda$  is the Coriolis parameter, with  $\Omega$  and  $\lambda$  being, correspondingly, the Earth's rotation rate and latitude. According to the solution, the mean horizontal current spirals clockwise and decays exponentially with depth. At the surface, the velocity is directed at  $45^\circ$  to the right (northern hemisphere) or the left (southern hemisphere) of the wind direction.

### 1.2 Limitations of the Ekman solution

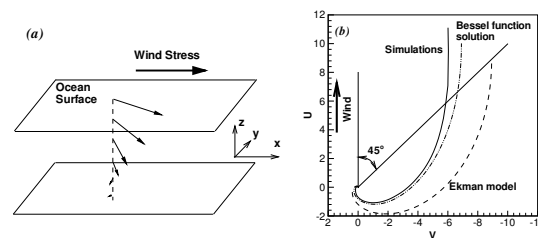
Simple, elegant, and clearly supported by laminar laboratory experiments, the Ekman model is, however, rather dissimilar to the actual turbulent flow near the ocean or lake surface. The basic assumption of Ekman's model of a steady-state wind and absence of any geostrophic currents are never completely realized in the open ocean. Some limitations of Ekman's solution include:

- The wind on the ocean surface is **never** steady.
- The effect of stratification is ignored.
- Eddy viscosity was assumed to be constant.
- The “ $f$ -plane” approximation neglects the influence of the horizontal (tangential to the Earth surface) component of the Earth rotation vector (i.e. dependence of latitude and wind direction).

In fact, a persistent well-developed Ekman spiral has, probably, never been observed in field measurements (see Price & Sundermeyer 1999 for a review). Attempts have been made to sort out the Ekman layer component of the measured data (see, e.g., Price, Weller, & Schudlich 1987, Chereskin & Roemmich 1991, Gnanadesikan & Weller 1995, Price & Sundermeyer 1999). Other oceanic flow features, such as Langmuir circulation and Stokes drift, further complicate matters.

## 2 Methodology

### 2.1 Problem Geometry



In the classic Ekman solution, the direction of the surface current forms an angle of  $45^\circ$  with the wind. The Bessel function solution can be found in Zikanov, Slinn, and Dhanak (2002).

### 2.2 Governing Equations

To non-dimensionalize the unsteady, incompressible, constant density Navier-Stokes equations, we use the surface friction velocity  $u_* = (\tau_0/\rho_0)^{1/2}$  as the typical velocity scale. Here,  $\tau_0$  is the RMS wind stress applied at the surface and  $\rho_0$  is the constant fluid density. For time scale, we use the reciprocal Coriolis parameter  $1/f = 1/2\Omega \sin \lambda$  ( $\Omega$  is the angular velocity of the Earth's rotation). The turbulent length  $L = u_*/f$  is used as the length scale, and  $\tau_0$  serves as the scale for pressure  $p$  and the turbulent stresses  $\tau_{ik}$ .

$$\frac{\partial u}{\partial t} + \mathbf{u} \cdot \nabla \mathbf{u} = -\frac{\partial p}{\partial x} + \frac{\partial \tau_{1k}}{\partial x_k} + v - 2\Omega_{\tau y} w \quad (3)$$

$$\frac{\partial v}{\partial t} + \mathbf{u} \cdot \nabla \mathbf{v} = -\frac{\partial p}{\partial y} + \frac{\partial \tau_{2k}}{\partial x_k} - u + 2\Omega_{\tau x} w \quad (4)$$

$$\frac{\partial w}{\partial t} + \mathbf{u} \cdot \nabla \mathbf{w} = -\frac{\partial p}{\partial z} + \frac{\partial \tau_{3k}}{\partial x_k} - 2\Omega_{\tau x} v + 2\Omega_{\tau y} u \quad (5)$$

$$\frac{\partial u}{\partial x} + \frac{\partial v}{\partial y} + \frac{\partial w}{\partial z} = 0 \quad (6)$$

### 2.3 Boundary Conditions

The flow is assumed to be statistically homogeneous in a horizontal plane. Therefore, the lateral boundaries are specified as being periodic. The upper surface is modeled as a rigid lid, with a constant wind-induced shear stress in the  $x$ -direction.

$$w = 0, \quad \tau_{13} = \tau_0, \quad \tau_{23} = 0 \quad \text{at} \quad z = L_z. \quad (7)$$

At the bottom of the computational domain we impose the free-slip conditions:

$$w = \tau_{13} = \tau_{23} = 0 \quad \text{at} \quad z = 0. \quad (8)$$

### 2.4 Numerical Method

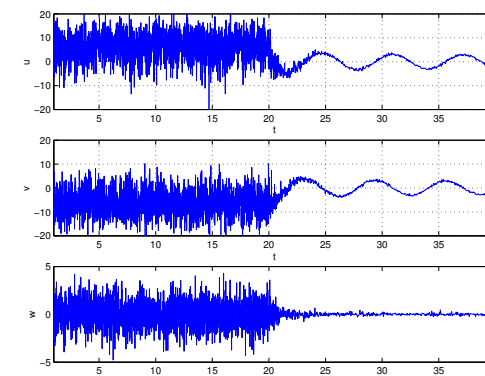
In the two horizontal directions, the periodic boundary conditions allow using the highly efficient Fourier pseudo-spectral technique based on the Fast Fourier Transform. Aliasing errors are removed using the 2/3-rule technique. In the vertical direction, the computational nodes are clustered near the upper surface. The  $z$ -coordinate is transformed according to

$$\zeta = \exp\left(\frac{z - L_z}{Z}\right), \quad (9)$$

where  $Z \leq L_z$  is a constant stretching parameter. In the transformed coordinate, the equations are discretized using the 2nd order central differences on a staggered grid. More details on the clustered grid technique used in this work can be found in Slinn & Riley (1998). Time integration is handled by a variable time-step third order Adams-Bashforth method. The dynamic model is used to model the subgrid stresses.

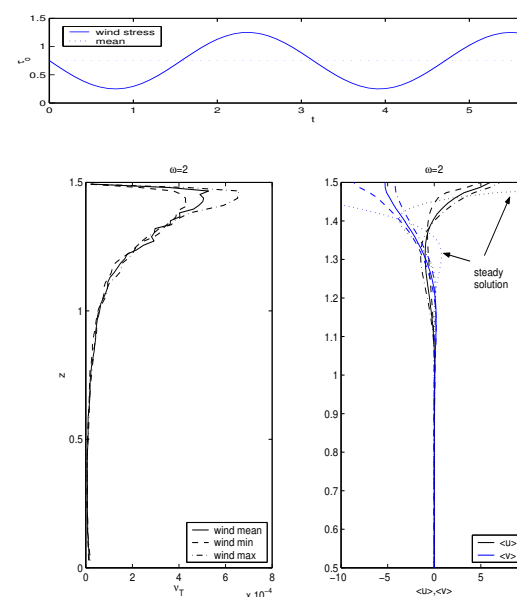
## 3 Results

### 3.1 Sudden cessation of the wind

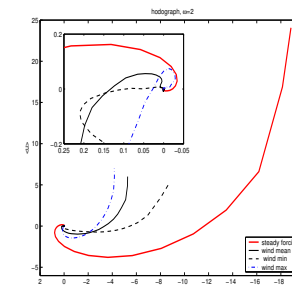


Here you can see the effect of stopping the wind stress after  $t = 20$  for the  $u$  and  $v$  components at a point on the surface, and for  $w$  at a point just below the surface. Without the wind stress, the turbulence levels (and the Ekman spiral!) quickly decay, leaving only inertial oscillations.

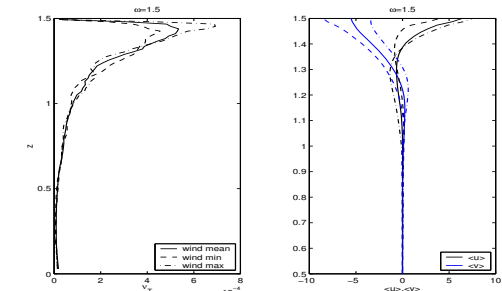
### 3.2 Forcing at twice the inertial frequency



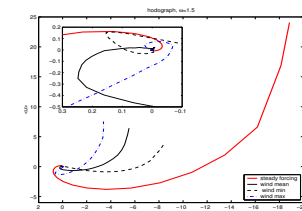
When forced at  $2 \times$  the inertial frequency, a weaker Ekman spiral is formed (see hodograph below). However, the depth of the spiral is similar to that of the steady solution.



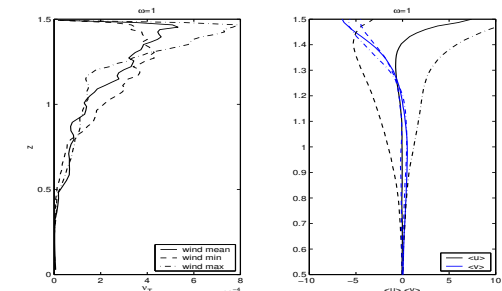
### 3.3 Forcing at $1.5 \times$ the inertial frequency



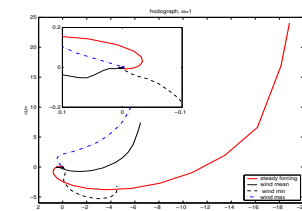
Forced at 1.5 times the inertial frequency, an even weak Ekman spiral is formed. At certain phases of forcing, the Ekman spiral becomes “unwound” (see inset).



### 3.4 Forcing at the inertial frequency



When forced at the inertial frequency, no Ekman spiral is formed. In fact, during phases of minimum forcing,  $\langle u \rangle$  becomes negative, indicating flow opposite to the wind direction. Note however, that the boundary layer has become thicker than when an Ekman spiral is present.



## 4 Conclusions

- Transition from a steady wind with an Ekman layer to no wind and inertial oscillations occurs quickly.
- Forcing at the inertial frequency results in surface transport opposite to the wind direction at times of minimum wind, and an overall increase in the thickness of the boundary layer.
- Monochromatic wind stress forcing can cause a breakdown of the Ekman spiral.